

Article

Effect of Shellac Waterborne Coating Microcapsules on the Optical, Mechanical and Self-Healing Properties of Waterborne Primer on *Tilia europaea* L. Wood

Xiaoxing Yan ^{1,2,*}, Yu Tao ² and Yijuan Chang ²

¹ Co-Innovation Center of Efficient Processing and Utilization of Forest Resources, Nanjing Forestry University, Nanjing 210037, China

² College of Furnishings and Industrial Design, Nanjing Forestry University, Nanjing 210037, China; taoyu@njfu.edu.cn (Y.T.); changyijuan@njfu.edu.cn (Y.C.)

* Correspondence: yanxiaoxing@njfu.edu.cn

Abstract: Microcapsules of melamine formaldehyde-coated shellac and waterborne coating were prepared by in situ polymerization at 400, 600, 800 and 1000 rpm. The microcapsules prepared at four different stirring rates were added into the waterborne primer at a concentration of 5.0%, 10.0%, 15.0%, 20.0% and 25.0%. The effects of microcapsules prepared at different stirring rates and the concentration of microcapsules added into the paint film on the optical, mechanical and liquid resistance properties of the paint film were investigated. The results showed that the comprehensive performance of *Tilia europaea* L. waterborne primer film was the best when the concentration of microcapsules obtained at 600 rpm was 5.0%. On this basis, the aging resistance and self-healing performance of waterborne primer film on *Tilia europaea* L. with the best comprehensive performance were explored to lay the foundation for optimizing the preparation process of self-healing coating.

Keywords: self-healing microcapsule; stirring rate; waterborne primer; wood coatings



Citation: Yan, X.; Tao, Y.; Chang, Y. Effect of Shellac Waterborne Coating Microcapsules on the Optical, Mechanical and Self-Healing Properties of Waterborne Primer on *Tilia europaea* L. Wood. *Coatings* **2021**, *11*, 785. <https://doi.org/10.3390/coatings11070785>

Academic Editor: Bojana Boh Podgornik

Received: 10 June 2021
Accepted: 26 June 2021
Published: 30 June 2021

Publisher's Note: MDPI stays neutral with regard to jurisdictional claims in published maps and institutional affiliations.



Copyright: © 2021 by the authors. Licensee MDPI, Basel, Switzerland. This article is an open access article distributed under the terms and conditions of the Creative Commons Attribution (CC BY) license (<https://creativecommons.org/licenses/by/4.0/>).

1. Introduction

In recent years, inspired by the phenomenon of biological self-healing, the concept of self-healing based on microcapsules has begun to show great potential in gel materials [1,2]. When micro-cracks appear in the coating, they can be repaired automatically by the self-healing technology of microcapsules [3–5], and the performance of the coating can even be improved [6]. The self-healing microcapsule technology has been introduced into the field of wood coatings [7]. Once the coating is damaged, the core material repair agent in the microcapsule will flow out, so as to achieve the purpose of repairing coating cracks [8], thus improving the usability and safety of wood coatings.

In the research on microcapsule preparation process optimization, Ma et al. [9] optimized the emulsification method and prepared probiotic microcapsules with milk protein as wall material. The results of orthogonal tests showed that the best microcapsule performance was obtained when the concentration of skimmed milk was 35%, the emulsification time was 10 min and the stirring speed was 600 rpm. Khodabakhshaghdam et al. [10] explored the effect of stirring rate on the performance of alginate chitosan (AC) core-shell microcapsules in a small stirred bioreactor. Fan et al. [11] prepared a series of microcapsules with polyurea formaldehyde as shell material and glass beads as core material, and systematically studied the effects of initial pH value, wall material concentration, surfactant concentration and stirring rate on the microencapsulation state. It was found that the final pH value and stirring rate were the main factors affecting the surface morphology of microcapsules. The stirring rate determines the shear force in the process of microcapsule preparation. If in the microencapsulation process, the shear force applied exceeds the Laplace pressure in the emulsion droplet, and the droplet will break [12–14]. It is

obvious that the stirring rate has an important effect on the formation of microcapsules. Zhang et al. [15] added the microcapsules with polyurea wall material and epoxy-ester core material to the epoxy coating to prepare the self-healing coating. The self-healing coating was proved to have good self-healing performance and good corrosion resistance to salt spray, by scanning electron microscopy and electrochemical impedance spectroscopy. Wang et al. [16] analyzed the mechanical properties of a self-healing coating with microcapsules. The results showed that microencapsulation had little effect on the mechanical properties of self-healing coating. Wang et al. [17] prepared self-healing coating by adding 10.0% concentration of microcapsules into an epoxy polyamine coating matrix, and explored the effect of microcapsules on the corrosion resistance of the self-healing coating. Mixing microcapsules into the coating will have a certain impact on the performance of the coating [18,19]. The more microcapsules are added, the better the repair effect is, but an excessive amount of microcapsules will affect the optical [20], mechanical [21], liquid and aging resistance [22] of *Tilia europaea* L. paint film. Waterborne primer is the first layer of paint film, which plays the role of protecting and sealing the substrate. The amount of microcapsules has a great influence on the primer [23–25].

Tilia europaea L. is wear-resistant, the structure of intercellular matrix is uniform and dense, and the texture is light and soft, so it is not easy to crack and deform [26]. The wood grain is beautiful, easy to process and has strong toughness. It can be used to make wood thread, blockboard, wooden crafts and other decorative materials [27,28]. Therefore, *Tilia europaea* L. was selected as the wood substrate for the experiment [29]. In-situ polymerization is one of the most commonly used methods to prepare microcapsules. The core material is the dispersed phase. The wall material prepolymer is soluble in a single phase, and its polymer is insoluble in the whole system. Therefore, the polymerization takes place on the dispersed phase core material to form microcapsules.

Shellac is a kind of purple natural resin secreted by lac insects after absorbing the sap of host tree. It mainly contains shellac resin, shellac wax and shellac pigment. Shellac resin has strong adhesion, good luster, and can be cured at room temperature. It is cheap, but its water resistance is poor. Waterborne acrylic coatings have good transparency and won't cover the original wood grain, but they are expensive, show poor chemical resistance and easily wear. Therefore, the mixture of shellac and waterborne acrylic coating was used as the core material of microcapsules. In this paper, the melamine formaldehyde (MF) resin coated shellac and waterborne coating microcapsules were prepared by in-situ polymerization. The effects of the amount of MF resin coated shellac and waterborne coating microcapsules prepared at different stirring rates on the optical, mechanical and liquid resistance properties of *Tilia europaea* L. primer film were discussed. At the same time, the aging resistance and repair properties of *Tilia europaea* L. primer film with the best concentration of microcapsules were explored. The purpose of this paper is to explore the influence of microcapsule type and concentration on the optical, mechanical, liquid resistance, aging resistance and self-healing properties of wood surface waterborne primer, and to provide the basis for optimizing the preparation process parameters of self-healing coating.

2. Materials and Methods

2.1. Experimental Materials

The basic information and sources of materials required in the experiment are shown in Table 1. Among them, the main components of waterborne primer are waterborne acrylic copolymer dispersion, matting agent, additive and water, and the solid content is about 30.0%. The components of shellac are shellac resin, shellac pigment, shellac wax, sugar and protein, etc.

Table 1. List of experimental materials.

Experimental Materials	Molecular Mass (g/mol)	CAS	Manufacturer
37.0% Formaldehyde	30.03	50-00-0	Jining Hengtai Chemical Co., Ltd., Jining, China
Melamine	126.15	108-78-1	Henan Ningjie Chemical Products Co., Ltd., Zhengzhou, China
Triethanolamine	149.19	102-71-6	Henan Yuheng Chemical Co., Ltd., Zhengzhou, China
Sodium dodecyl benzene sulfonate (SDBS)	348.48	25155-30-0	Xi'an Tianmao Chemical Co., Ltd., Xi'an, China
Citric acid monohydrate	210.14	5949-29-1	Nanjing Chemical Reagent Co., Ltd., Nanjing, China
Anhydrous ethanol	46.07	64-17-5	Tianjin Fuyu Fine Chemical Co., Ltd., Tianjin, China
<i>Tilia europaea</i> L. (100 mm × 65 mm × 4 mm)	-	-	Guangdong Yihua Life Science and Technology Co., Ltd., Guangzhou, China
Waterborne primer	-	-	Dulux (Changzhou) Co., Ltd., Changzhou, China
Shellac	-	-	Jinan Dahui Chemical Technology Co., Ltd., Jinan, China
15.0% NaCl solution	-	-	Self-made
70% Medical ethanol	-	-	Qingdao Heinrich Innoway Disinfection Technology Co., Ltd., Qingdao, China
Detergent	-	-	Shanghai and Huangbai Cat Co., Ltd., Shanghai, China
Red ink	-	-	Shanghai Fine Cultural Products Co., Ltd., Shanghai, China

2.2. Preparation of Microcapsules

First, melamine: formaldehyde: water was mixed in a 250 mL beaker at a mass ratio of 1:2:5. Triethanolamine was added dropwise to adjust the pH value to 8.0–9.0. The mixture was stirred and heated in a 70 °C bain-marie until transparent, then an appropriate amount of distilled water was added. The wall material prepolymer was obtained by continuously stirring at 600 rpm for 30 min. The shellac and ethanol were dissolved in a mass ratio of 1:5, and the supernatant was extracted by centrifugation. The waterborne primer and shellac solution were mixed in a mass ratio of 1:1 and stirred evenly, and the emulsifier (sodium dodecylbenzene sulfonate aqueous solution) was added to the mixture of shellac and waterborne coating. The composite was reacted with 60 min in 70 °C constant temperature bain-marie to obtain the core material emulsion. The wall material was slowly added to the core material emulsion and the mixture was placed in DF-101Z collector constant temperature heating magnetic stirrer at four different speeds of 400 rpm, 600 rpm, 800 rpm and 1000 rpm, respectively. After the pH value was regulated to 2.5–3.0 with citric acid, the mixture was slowly heated to 70 °C for 3 h. After standing for 7 days, the mixture was filtered by SHZ-D circulating water multi-purpose vacuum pump (Henan Yuhua Instrument Co., Ltd., Zhengzhou, China), and then the product was put into a 40 °C DHG-9643BS-BS-III electric constant temperature blast drying oven (Shanghai Xinmiao Medical Instrument Manufacturing Co., Ltd., Shanghai, China) to dry for 48 h. The yellow powder obtained is melamine formaldehyde coated shellac waterborne coating microcapsule.

2.3. Preparation of Waterborne Coatings

First of all, *Tilia europaea* L. boards were placed at 20 °C and relative humidity of 50.0% ± 5.0% to reach equilibrium moisture concentration in a week. Four kinds of microcapsules prepared at different stirring rates (400, 600, 800 and 1000 rpm) were added to the waterborne primer respectively to prepare self-repairing waterborne coatings with microcapsule concentration of 5.0%, 10.0%, 15.0%, 20.0% and 25.0%, respectively. The prepared coating was applied on the surface of *Tilia europaea* L. substrate by a SZQ tetrahedral preparator (Dongguan Huaguo Precision Instrument Co., Ltd., Dongguan, China), and the film was dried at room temperature for 30 min, then polished with 800 mesh sandpaper

and wiped with dry cloth. The above process was duplicated twice. The thickness of dry waterborne primer coating was about 60 μm .

2.4. Testing and Characterization

A taper hole with a top angle of 120° was drilled on the tested paint film, and the hole wall was imaged in a $40\times$ measuring microscope. The microscope was focused on the bus bar perpendicular to the main optical axis, and the length of the paint film part of the bus bar was measured by the micrometer device of the microscope (Guangzhou Xingzhen Technology Co., Ltd., Guangzhou, China). Then the coating thickness was calculated according to the functional relationship, that is, the coating thickness was half of the length of the paint film part on the bus bar. Three measuring points were selected for each sample, and the dry film thickness was obtained by three-point arithmetic average method.

A Zeiss Axio scope A1 optical microscope (OM) supplied by Guangzhou Xingzhen Technology Co., Ltd. (Guangzhou, China) and a quanta-200 scanning electron microscope (SEM), provided by FEI Company (Hillsboro, OR, USA) were applied to show the morphology of the microcapsules prepared at different stirring rates and waterborne primer film. The microcapsule samples were attached to the sample disk by a conductive adhesive, and the sample was plated with gold using a certain time and voltage. After the gold plating, the sample disk was put into the sample room. When the vacuum value reached a certain value, the SEM image of the sample can be observed.

The chemical composition of microcapsule and waterborne primer film was analyzed by a Vertex 80V Fourier transform infrared spectroscopy (FTIR) Instrument from Shanghai smio Analytical Instrument Co., Ltd. (Shanghai, China). An attenuated total reflection (ATR) device was used to measure the infrared spectrum of the coating. The samples were placed on the test bench and fixed on the top surface of the pure diamond crystal with a pressure bar. The infrared spectra of microcapsules were determined by the KBr method. KBr (200 mg) and microcapsules (1–2 mg) were put into the grinding dish to grind fully to avoid uneven particles. After grinding, the samples were put into the mold with medication spoon, and the mold was placed on the tablet press. After the pressure reached 20 MPa, the mold was taken out, and the internal module was put into the tablet rack to determine the infrared spectrum of the microcapsule powder.

A SEGT-J portable color difference meter (Shenyang Guoti precision testing instrument Co., Ltd., Shenyang, China) was used to measure the color value of the waterborne primer film on the surface of *Tilia europaea* L., and the color difference value (ΔE^*) of the film before and after adding microcapsules was calculated. L^* represented brightness, a^* represented red and green, b^* represented yellow and blue, c^* represented degree of color saturation, and H^* represented hue. The color difference (ΔE^*) can be calculated according to the formula:

$$\Delta E^* = [(\Delta L^*)^2 + (\Delta a^*)^2 + (\Delta b^*)^2]^{1/2}$$

The gloss of the paint film was measured by a HG268 intelligent gloss meter from Shenzhen Yuanyuan Instrument and Equipment Co., Ltd. (Shenzhen, China), and the gloss was recorded at three incidence angles of 20° , 60° and 85° . At normal atmospheric temperature, the liquid resistance of the coating with and without microcapsules was experimented, and NaCl, ethanol, dishwashing liquid and red ink were selected as the liquid resistance reagents.

A pencil hardness tester (Dongguan Huaguo Precision Instrument Co., Ltd., Dongguan, China) was used to measure the hardness of the paint film with 6H-6B pencil. A QFH-HG 600 film scribbler (Dongguan Huaguo Precision Instrument Co., Ltd., Dongguan, China) was employed to test the film adhesion. The multi blade cutter was perpendicular to the plate and cuts the coating at a certain speed under a certain pressure to draw a grid pattern. Then the tape was pasted on the whole grid and taken out at the minimum angle. The magnifying glass was used to observe the damage of the coating and the adhesion level of the coating was judged according to the damage.

The impact resistance of paint film was tested by QCJ film impactor, which was provided by Tianjin Jinghai Kexin Testing Machine Factory (Tianjin, China). A AG-IC100KN precision electronic universal testing machine produced by Shimadzu Co., Ltd. (Kyoto, Japan) was applied to survey the tensile strength of the coating. The two ends of the film were fixed with clamps, and the film was stretched at the speed of 0.12 mm/min, and the film broke under a certain longitudinal load. L_0 was the initial value of the distance between the clamps, and L_a was the distance when the clamps break. The elongation at break (e) of paint film can be calculated by the following formula:

$$e = (L_a - L_0) / L_0 \times 100\%$$

The coatings without microcapsules and with 5.0% microcapsules prepared at 600 rpm on *Tilia europaea* L. board were placed in the ZN ultraviolet weather resistance tester for 24 h (Nanjing Environmental Test Equipment Co., Ltd., Nanjing, China) for aging and stability tests. The UV light with the wavelength of 280~340 nm was used in the aging test. The light source was eight 40 W rated ultraviolet fluorescent tubes, which were distributed on both sides of the machine. The distance between the sample surface and the UV lamp plane was 50 mm. The illumination temperature was 60 °C, the condensation temperature was 50 °C, and the cycle time was 4 h. The color difference and gloss of the film before and after aging were checked, and the SEM and FTIR of the film before and after aging were analyzed.

The cutter blade was used to scratch the paint film, and the OM was used to observe the self-repairing situation of the paint film for 7 days. After slicing the side of *Tilia europaea* L. coated with waterborne coating, the interface mechanism between the microcapsule and *Tilia europaea* L. was observed by the OM. $A_{original}$ was the original width of the crack, and A_{healed} was the width of the repaired crack. The repair rate (σ) of cracks can be calculated by the following formula:

$$\sigma = (A_{original} - A_{healed}) / A_{original} \times 100\%$$

All the tests were repeated four times with an error of less than 5.0%.

3. Results and Discussion

3.1. Morphology and Composition Analysis of Microcapsules

The OM and SEM images of microcapsules prepared at different stirring rates are shown in Figures 1 and 2. It can be seen from Figure 1 that the four kinds of microcapsules have different areas of dark color and light color, indicating that the composition of wall material and core material is different, and the absorption and reflection of light source are also different. The bright spots in the inner layer represent the core material, and the dark rings in the outer layer represent the wall material, forming a shell-core structure. Figure 2A shows the microcapsules prepared at the stirring rate of 400 rpm. The particle size of the microcapsules varies from large to small. The agglomeration of the larger microcapsules is obvious, and more small microcapsules are attached on the surface. Figure 2B shows the microcapsules prepared at 600 rpm stirring rate. The most of microcapsules are complete sphere with smooth surface, and the particle size is basically uniform. The obtained microcapsules are good. Figure 2C shows the microcapsules prepared at 800 rpm stirring rate. The particle size is basically the same, but the dispersion is poor. Figure 2D shows the microcapsules prepared at the stirring rate of 1000 rpm, with serious agglomeration, irregular spherical shape and slightly rough surface. With the rise of stirring speed and shear force, the particle size of microcapsules decreases gradually, and the microcapsules with the best morphology are prepared when the stirring speed is 600 rpm. Figure 3 shows the size distribution of the microcapsules prepared at 600 rpm. Most of the microcapsules were in the range of 6–8 μm .

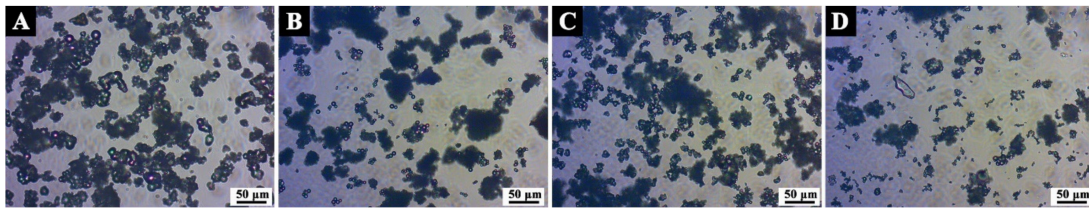


Figure 1. The OM morphology of microcapsules prepared at different stirring rates: (A) 400 rpm, (B) 600 rpm, (C) 800 rpm, (D) 1000 rpm.

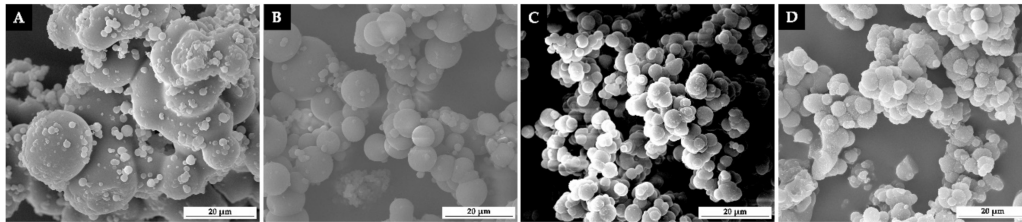


Figure 2. The SEM morphology of microcapsules prepared at different stirring rates: (A) 400 rpm, (B) 600 rpm, (C) 800 rpm, (D) 1000 rpm.

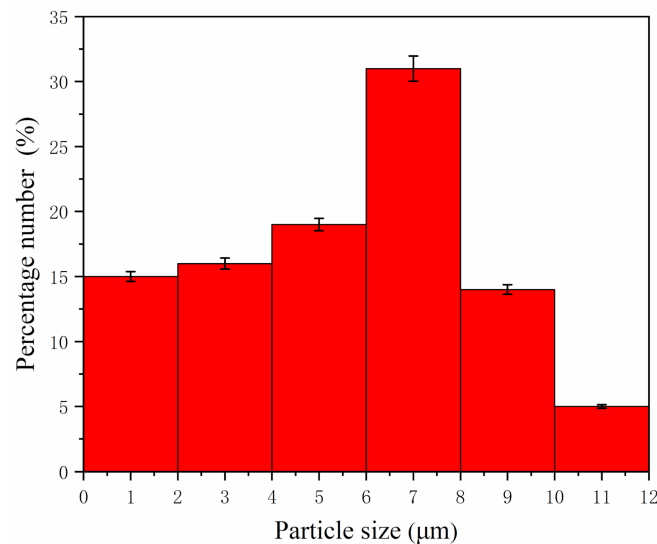


Figure 3. Particle size distribution of microcapsules prepared at 600 rpm.

The FTIR of microcapsules prepared at different stirring rates are shown in Figure 4. The 1726 cm^{-1} symbolizes the characteristic peak of C=O in the waterborne acrylic resin coating, and the 1750 cm^{-1} is the stretching vibration of –COOH group in shellac [30]. The two peaks overlapped in the infrared curves of microcapsules prepared at four different stirring rates, and a wide peak was formed in the range of $1750\text{ cm}^{-1}\sim 1650\text{ cm}^{-1}$. At the same time, the color of microcapsule powder was yellow, which indicated that the core material shellac was coated successfully. The 3343 cm^{-1} is the stretching vibration of N–H group in MF resin [31]. The microcapsules prepared with four different stirring rates also showed this peak, which indicated that MF resin existed in the microcapsules. Because the peak value trend of microcapsules prepared at four different stirring rates is basically the same, it shows that the four microcapsules have the same composition, and the microcapsules have been successfully prepared.

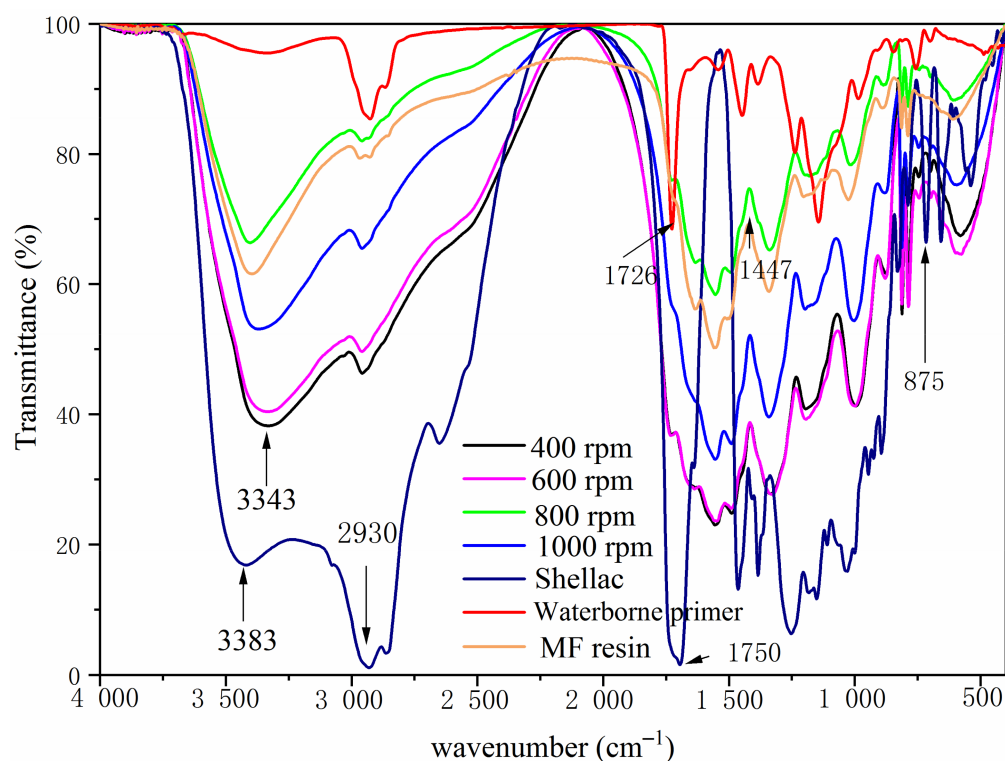


Figure 4. The FTIR of microcapsules prepared by different stirring rates.

3.2. Effect of Microcapsule on the Optical Properties of Surface Coating on *Tilia europaea* L. Wood

Figure 5 shows that the color difference (ΔE^*) of *Tilia europaea* L. primer film added with microcapsules prepared at four different stirring rates goes up with the rise of microcapsule concentration, which is due to the uneven distribution of microcapsules. On the whole, the color difference value of the film with 5.0% microcapsules prepared at 600 rpm stirring rate is the smallest.

Table 2 shows the effect of different concentration of microcapsules prepared at different stirring rates on the gloss of waterborne primer film. The gloss of paint film at 60° incident angle is shown in Figure 6. At the same stirring rate, the gloss of the film decreased with the rise of microcapsule concentration. When the concentration of microcapsule was 5.0%, the gloss of the film was relatively high. When the concentration of microcapsule was 10.0% or more, the gloss of the film was relatively low and the difference was not obvious. This is because with the enhancement of microcapsule particles in the film, the diffuse reflection of the film surface is enhanced, which reduces the gloss of the film.

Table 2. Effect of microcapsule concentration with different stirring rates on gloss of waterborne primer.

Stirring Rate (rpm)	Microcapsule Concentration (%)	20° Gloss (%)	60° Gloss (%)	85° Gloss (%)
400	0	4.9 ± 0.1	20.2 ± 0.5	19.6 ± 0.6
	5.0	1.7 ± 0	9.1 ± 0.2	7.2 ± 0.2
	10.0	1.0 ± 0	2.2 ± 0	0.3 ± 0
	15.0	1.1 ± 0	1.6 ± 0	0.2 ± 0
	20.0	1.1 ± 0	1.3 ± 0	0.1 ± 0
	25.0	1.1 ± 0	1.4 ± 0	0.1 ± 0

Table 2. Cont.

Stirring Rate (rpm)	Microcapsule Concentration (%)	20° Gloss (%)	60° Gloss (%)	85° Gloss (%)
600	5.0	1.8 ± 0	8.4 ± 0	2.4 ± 0
	10.0	1.1 ± 0	2.4 ± 0	0.3 ± 0
	15.0	1.1 ± 0	1.6 ± 0	0.2 ± 0
	20.0	1.0 ± 0	1.2 ± 0	0 ± 0
	25.0	1.2 ± 0	1.4 ± 0	0 ± 0
800	5.0	1.2 ± 0	1.4 ± 0	0.2 ± 0
	10.0	1.1 ± 0	1.4 ± 0	0.1 ± 0
	15.0	1.2 ± 0	1.3 ± 0	0.2 ± 0
	20.0	1.1 ± 0	1.4 ± 0	0 ± 0
	25.0	0.9 ± 0	1.2 ± 0	0 ± 0
1000	5.0	1.3 ± 0	1.6 ± 0	0.1 ± 0
	10.0	1.0 ± 0	1.5 ± 0	0.1 ± 0
	15.0	1.1 ± 0	1.4 ± 0	0 ± 0
	20.0	1.1 ± 0	1.2 ± 0	0.1 ± 0
	25.0	1.1 ± 0	1.2 ± 0	0 ± 0

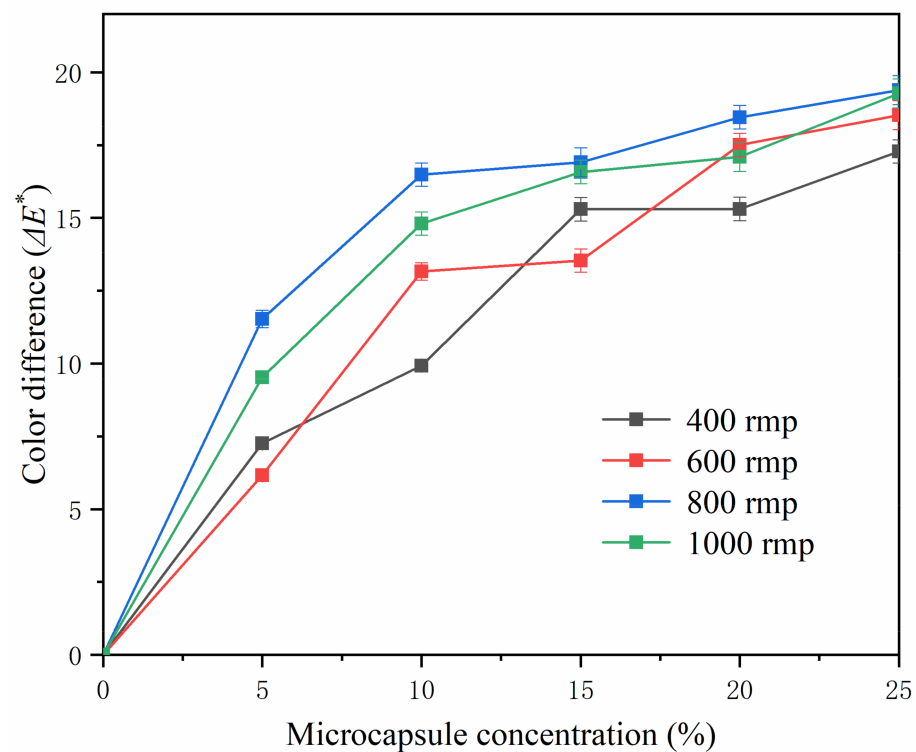


Figure 5. Effect of microcapsules on the color difference of waterborne primer coating.

3.3. Effect of Microcapsules on the Mechanical Properties of Surface Coating on *Tilia europaea* L. Wood

The results of the influence of different concentration microcapsules prepared at different stirring rates on the elongation at break of the film are shown in Figure 7. It can be seen that with the rise of microcapsule concentration, the elongation at break of the film decreases gradually, which is because with the rise of microcapsule concentration, the film is more prone to embrittlement. The microcapsules with 5.0% concentration and prepared at 600 rpm stirring rate had the highest elongation at break. Because the particle size of the microcapsules prepared at the stirring rate of 600 rpm is uniform, it can enhance the flexibility of the film.

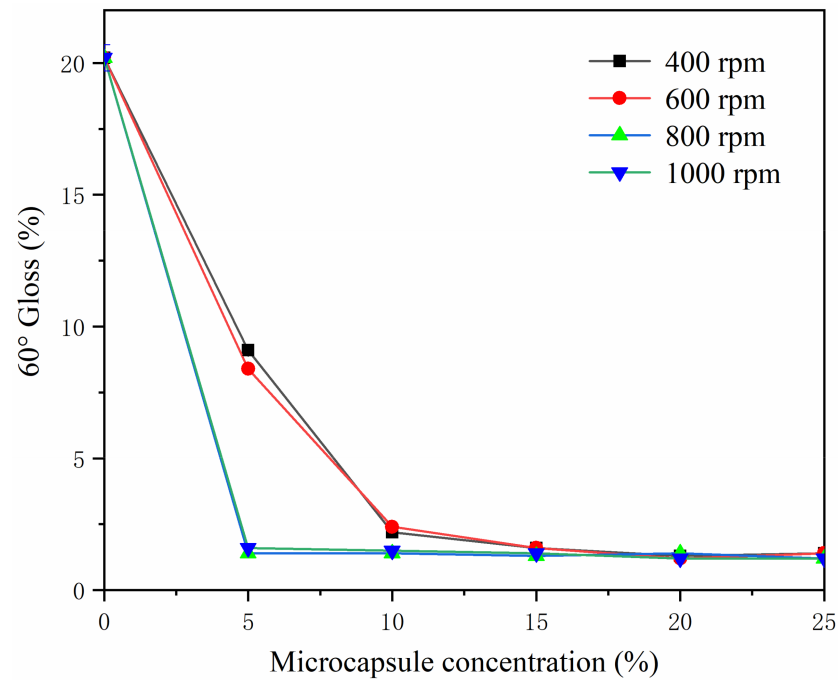


Figure 6. Effect of microcapsules on the gloss.

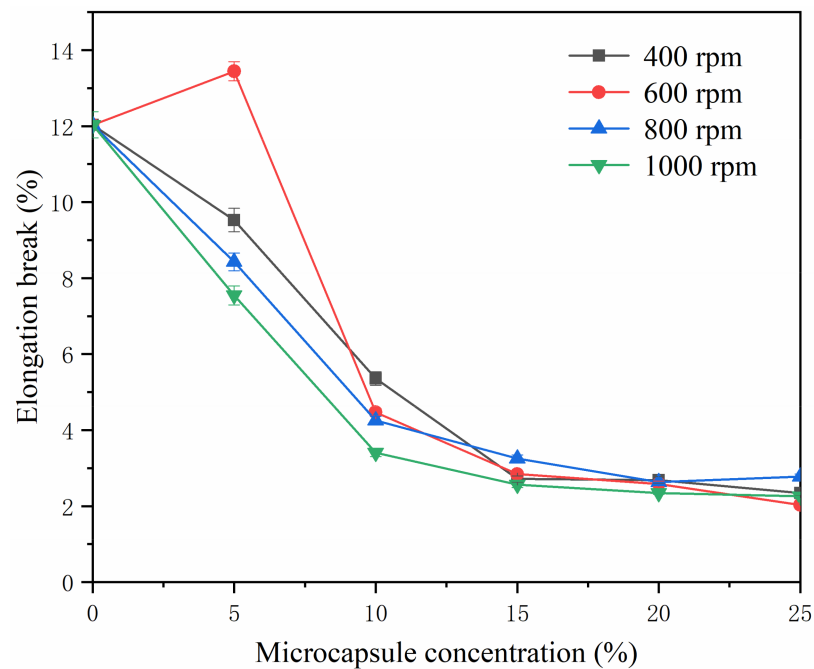


Figure 7. Effect of the microcapsules on the elongation at break.

As can be seen in Table 3, when the amount of microcapsules increased gradually, the adhesion grade of the coating film gradually decreased. Compared with other stirring rates, the adhesion of microcapsule coating obtained at 600 rpm is better.

The result showed that the adhesion of the film with 5.0% microcapsule was better, which was grade 0 and grade 1. When the concentration of microcapsules prepared at 600 rpm, 800 rpm and 1000 rpm was 10.0% and 15.0%, respectively, the film adhesion was good, which was grade 1. The film with 20.0% and 25.0% microcapsules prepared at 400 rpm had the worst adhesion. The reason is that the stirring rate is too slow in the preparation of microcapsules, which will lead to large and uneven microcapsule particles.

When the microcapsule and waterborne coating are mixed and applied on the surface of wood, the contact area between the microcapsule and wood is different, resulting in poor adhesion between layers.

Table 3. Effect of microcapsule concentration with different stirring rates on adhesion of waterborne primer film.

Microcapsule Concentration (%)	Adhesion (Grade)			
	Stirring Rate 400 rpm	Stirring Rate 600 rpm	Stirring Rate 800 rpm	Stirring Rate 1000 rpm
0	0 ± 0	0 ± 0	0 ± 0	0 ± 0
5.0	1 ± 0	0 ± 0	1 ± 0	1 ± 0
10.0	2 ± 0	1 ± 0	1 ± 0	1 ± 0
15.0	2 ± 0	1 ± 0	1 ± 0	1 ± 0
20.0	3 ± 0	2 ± 0	2 ± 0	2 ± 0
25.0	4 ± 0	2 ± 0	2 ± 0	2 ± 0

The influence of microcapsules prepared at different stirring rates on the film hardness of waterborne primer is shown in Table 4. The B is blackness, and the H is hardness. The more B number is, the softer it is, and the more H number is, the harder it is. It can be seen that under the same stirring rate, with the increased concentration of MF resin coated shellac waterborne coating microcapsules, the overall hardness of the coating film showed an upward trend. The overall hardness of the coating film with microcapsules prepared at 600 rpm was higher than that at other stirring rates. The film hardness was better when the concentration of microcapsules is 5.0% and 10.0%, respectively. The amount of microcapsules should not be too high, otherwise the gloss of the film will be reduced.

Table 4. Effect of concentration of microcapsules with different stirring rates on film hardness of waterborne primer.

Microcapsule Concentration (%)	Hardness			
	Stirring Rate 400 rpm	Stirring Rate 600 rpm	Stirring Rate 800 rpm	Stirring Rate 1000 rpm
0	HB ± 0	HB ± 0	HB ± 0	HB ± 0
5.0	4H ± 0	3H ± 0	4H ± 0	3H ± 0
10.0	5H ± 0	4H ± 0	3H ± 0	3H ± 0
15.0	3H ± 0	3H ± 0	3H ± 0	4H ± 0
20.0	H ± 0	4H ± 0	4H ± 0	4H ± 0
25.0	5H ± 0	3H ± 0	5H ± 0	5H ± 0

It can be seen from Table 5 that the impact resistance of the coating improves first and then decreases with the rise of the concentration of microcapsules. When the stirring rate was 1000 rpm and the amount of microcapsules was 10.0%, the impact resistance of *Tilia europaea* L. film was larger. Because the microcapsules prepared at 1000 rpm were small in size and dispersed evenly in the coating, the impact resistance of the film was larger. The film with microcapsule had higher impact resistance than that without microcapsule. The reason is that the increase of microcapsule particles on the surface of the film leads to the increase of the strength of the film to cope with the impact, but when the concentration of microcapsule in the film is too high, the performance of the film will be reduced, and it is difficult to resist the impact of external forces, so it is very easy to be damaged.

Table 5. Effect of concentration of microcapsules with different stirring rates on impact resistance of waterborne primer film.

Microcapsule Concentration (%)	Impact Resistance (kg·cm)			
	Stirring Rate 400 rpm	Stirring Rate 600 rpm	Stirring Rate 800 rpm	Stirring Rate 1000 rpm
0	5.0 ± 0	5.0 ± 0	5.0 ± 0	5.0 ± 0
5.0	5.0 ± 0	12.0 ± 0	19.0 ± 0	7.0 ± 0
10.0	9.0 ± 0	14.0 ± 0	21.0 ± 0.8	25.0 ± 0.8
15.0	8.0 ± 0	12.0 ± 0	13.0 ± 0	20.0 ± 0.8
20.0	7.0 ± 0	11.0 ± 0	10.0 ± 0	15.0 ± 0
25.0	7.0 ± 0	10.0 ± 0	10.0 ± 0	12.0 ± 0

3.4. Effect of Microcapsule on liquid Resistance of Surface Coating on *Tilia europaea* L. Wood

The influence of microcapsules prepared at different stirring rates and with different concentrations on the color difference (ΔE^*) of waterborne primer film before and after liquid resistance is shown in Table 6. The color difference of the film before and after liquid resistance with microcapsule was smaller than that without microcapsule, and with the enlargement of the concentration of microcapsule, the color difference of the film before and after liquid resistance first decreased and then increased. The coating with microcapsules prepared at 600 rpm had the smallest color difference before and after liquid resistance. The coating with microcapsule concentration of 5.0% and 10.0% had smaller color difference before and after liquid resistance to NaCl, ethanol and detergent, but the coating with microcapsule concentration of 10.0% had larger color difference before and after liquid resistance to red ink. Because microcapsules were a powder, the more microcapsules were added, the more colors would be absorbed. When the concentration of microcapsules prepared at 600 rpm in the film was 5.0%, the film had better liquid resistance.

Table 6. Effect of the concentration of microcapsules with different stirring rates on the color difference of waterborne primer film.

Stirring Rate (rpm)	Microcapsule Concentration (%)	NaCl	Ethanol	Detergent	Red Ink
400	0	50.2 ± 1.3	6.3 ± 0.2	12.0 ± 0.3	61.0 ± 1.5
	5.0	4.9 ± 0	5.3 ± 0.1	3.3 ± 0	47.8 ± 1.6
	10.0	6.2 ± 0.2	2.7 ± 0	6.7 ± 0.2	23.4 ± 0.5
	15.0	4.1 ± 0.1	4.8 ± 0.1	8.2 ± 0.2	63.8 ± 1.4
	20.0	6.1 ± 0.1	7.6 ± 0.2	9.8 ± 0.2	67.0 ± 1.8
	25.0	3.2 ± 0	3.6 ± 0	11.2 ± 0.2	52.7 ± 1.8
600	0	50.2 ± 1.4	6.3 ± 6.5	12.0 ± 0.3	61.0 ± 2.0
	5.0	4.2 ± 0.1	3.9 ± 0	3.1 ± 0	40.6 ± 1.3
	10.0	1.8 ± 0	2.5 ± 0	1.3 ± 0	3.9 ± 0
	15.0	1.7 ± 0	3.3 ± 0	2.1 ± 0	39.2 ± 1.5
	20.0	3.9 ± 0	4.1 ± 0.1	8.9 ± 0.2	29.9 ± 0.9
	25.0	12.9 ± 0.3	18.6 ± 0.5	18.8 ± 0.6	28.6 ± 1.3
800	0	50.2 ± 1.4	6.3 ± 0.2	12.0 ± 0.3	61.0 ± 1.3
	5.0	12.3 ± 0.3	14.7 ± 0.3	14.9 ± 0.4	14.4 ± 0.4
	10.0	2.8 ± 0	3.3 ± 0	10.1 ± 0.2	46.4 ± 1.0
	15.0	2.1 ± 0	7.3 ± 0.2	7.6 ± 0.1	52.4 ± 1.0
	20.0	7.0 ± 0	12.7 ± 0.5	7.2 ± 0.2	49.1 ± 1.5
	25.0	13.2 ± 0.2	10.6 ± 0.3	9.0 ± 0.1	32.8 ± 0.6

Table 6. Cont.

Stirring Rate (rpm)	Microcapsule Concentration (%)	NaCl	Ethanol	Detergent	Red Ink
1000	0	50.2 ± 1.7	6.3 ± 0.2	12.0 ± 0.3	61.0 ± 2
	5.0	5.6 ± 0.1	7.9 ± 0.1	5.3 ± 0	7.2 ± 0.1
	10.0	6.3 ± 0.2	8.9 ± 0.2	4.6 ± 0.1	5.7 ± 0.1
	15.0	5.4 ± 0.1	26.0 ± 0.8	7.0 ± 0.1	51.4 ± 1.5
	20.0	10.7 ± 0.2	5.8 ± 0.1	13.1 ± 0.3	32.3 ± 0.6
	25.0	6.9 ± 0.1	16.9 ± 0.5	28.5 ± 0.8	20.9 ± 0.4

The influence of microcapsules prepared at different stirring rates with different concentration on the gloss of waterborne primer film after liquid resistance is shown in Table 7, which shows the gloss of paint film at incidence angle of 60°. With the enhancement of the concentration of microcapsules, the gloss of the film after liquid resistance decreased. The coating after liquid resistance to red ink had lower gloss than that after liquid resistance to NaCl, ethanol and detergent. The reason is that the red pigment in the red ink is a kind of organic matter, and the color value of red is relatively large, so it is easy to adsorb on the surface of microcapsules.

Table 7. The gloss of waterborne primer film after liquid resistance.

Stirring Rate (rpm)	Microcapsule Concentration (%)	NaCl	Ethanol	Detergent	Red Ink
400	0	9.8 ± 0.2	9.6 ± 0.2	10.0 ± 0.2	11.7 ± 0.4
	5.0	6.4 ± 0.2	6.1 ± 0.1	7.6 ± 0.1	7.1 ± 0.2
	10.0	2.7 ± 0	2.6 ± 0	2.3 ± 0	2.1 ± 0
	15.0	1.5 ± 0	1.5 ± 0	1.5 ± 0	0.7 ± 0
	20.0	1.5 ± 0	1.5 ± 0	2.0 ± 0	0.6 ± 0
	25.0	1.4 ± 0	1.4 ± 0	1.6 ± 0	0.8 ± 0
600	0	9.8 ± 0.2	9.6 ± 0.1	10.0 ± 0.2	11.7 ± 0.4
	5.0	6.4 ± 0.1	5.2 ± 0.1	6.0 ± 0.1	5.3 ± 0.1
	10.0	2.0 ± 0	1.0 ± 0	2.6 ± 0	0.9 ± 0
	15.0	1.3 ± 0	1.0 ± 0	1.3 ± 0	1.4 ± 0
	20.0	1.5 ± 0	1.6 ± 0	1.5 ± 0	1.1 ± 0
	25.0	1.4 ± 0	1.4 ± 0	1.6 ± 0	1.7 ± 0
800	0	1.4 ± 0	1.4 ± 0	1.2 ± 0	0.9 ± 0
	5.0	1.4 ± 0	1.4 ± 0	1.5 ± 0	1.4 ± 0
	10.0	1.4 ± 0	1.4 ± 0	1.2 ± 0	0.9 ± 0
	15.0	1.6 ± 0	1.5 ± 0	1.8 ± 0	0.8 ± 0
	20.0	1.7 ± 0	1.6 ± 0	1.8 ± 0	0.8 ± 0
	25.0	1.7 ± 0	1.6 ± 0	1.8 ± 0	1.0 ± 0
1000	0	9.8 ± 0.2	9.6 ± 0.2	10.0 ± 0.2	11.7 ± 0.9
	5.0	1.6 ± 0	1.2 ± 0	1.7 ± 0	1.7 ± 0
	10.0	1.5 ± 0	1.6 ± 0	1.5 ± 0	1.4 ± 0
	15.0	1.7 ± 0	1.5 ± 0	1.7 ± 0	1.4 ± 0
	20.0	1.6 ± 0	1.5 ± 0	1.6 ± 0	1.0 ± 0
	25.0	1.5 ± 0	1.6 ± 0	1.5 ± 0	0.9 ± 0

3.5. Effect of Microcapsules on the Microstructure and Composition of Surface Coating on *Tilia europaea* L. Wood

Based on the optical, mechanical and liquid resistance properties of the coating film, it can be seen that the microcapsules prepared at 600 rpm stirring rate had a good effect on the comprehensive properties of wood surface waterborne primer. The SEM of waterborne primer film with different concentrations of microcapsules are shown in Figure 8. There were no particles on the surface of the film without microcapsules. There were obvious particles on the surface of the coating film with the concentration of 5.0% and 10.0%

microcapsules, and there is a little agglomeration between the particles (Figure 8B,C). There were a lot of particles in the coating film with the concentration of 25.0% microcapsules, and the agglomeration phenomenon was very serious (Figure 8D). With the increase of the concentration of microcapsules, the surface particles increased obviously, which was also the reason for the increase of color difference, the decrease of gloss and the change of mechanical properties. When the concentration of microcapsule was 5.0%, the microstructure of the film was better.

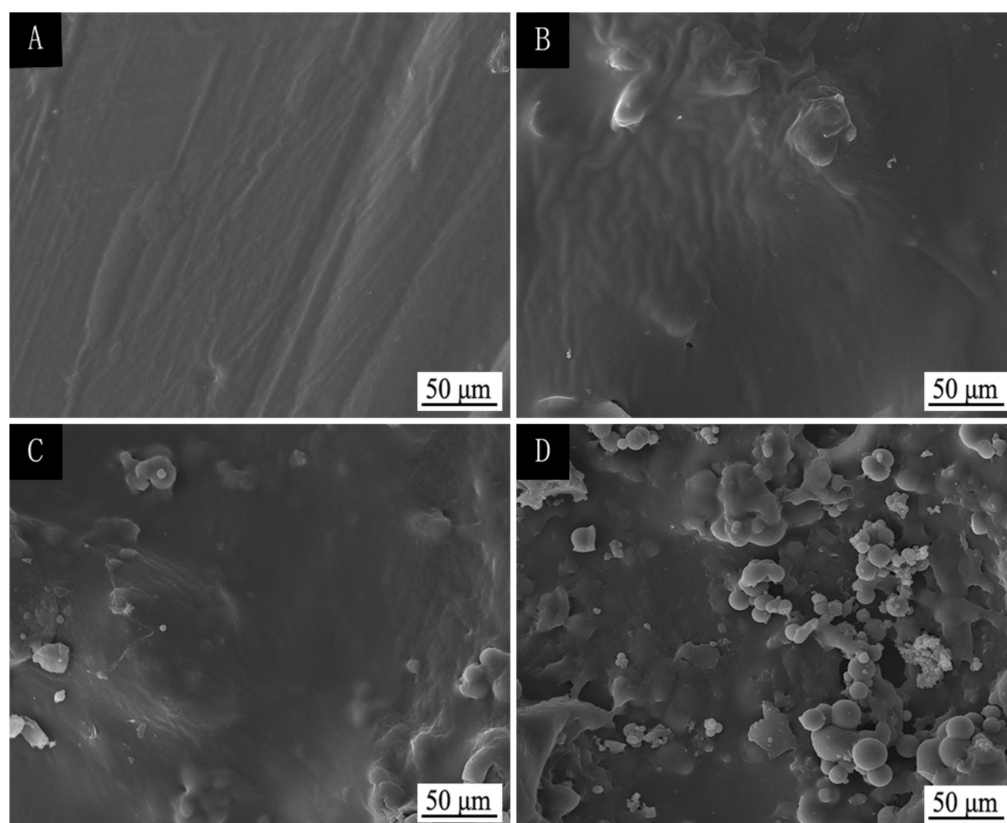


Figure 8. SEM of waterborne primer coating with different concentration of microcapsules (stirring rate 600 rpm): (A) 0; (B) 5.0%; (C) 10.0%; (D) 25.0%.

Figure 9 shows the FTIR of the film of microcapsules prepared at 600 rpm stirring rate with different concentrations. The characteristic absorption peaks of functional groups in each substance are shown in Table 8 [27,28]. The FTIR of the coatings with different concentration of microcapsules were basically the same, and no peak disappeared or appeared, which indicated that there was no chemical reaction between microcapsules and coatings.

Table 8. Assignment of infrared absorption peaks.

Peak Value	Functional Group	Substance
1447 cm ⁻¹ /2930 cm ⁻¹ /2865 cm ⁻¹	C-H	-
2930 cm ⁻¹ /2854 cm ⁻¹ /1450 cm ⁻¹	-CH ₂	-
1600 cm ⁻¹	C=N	MF resin
1542 cm ⁻¹ /3500–3300 cm ⁻¹	N-H	waterborne acrylic resin
1726 cm ⁻¹	C=O	shellac
1750 cm ⁻¹	-COOH	

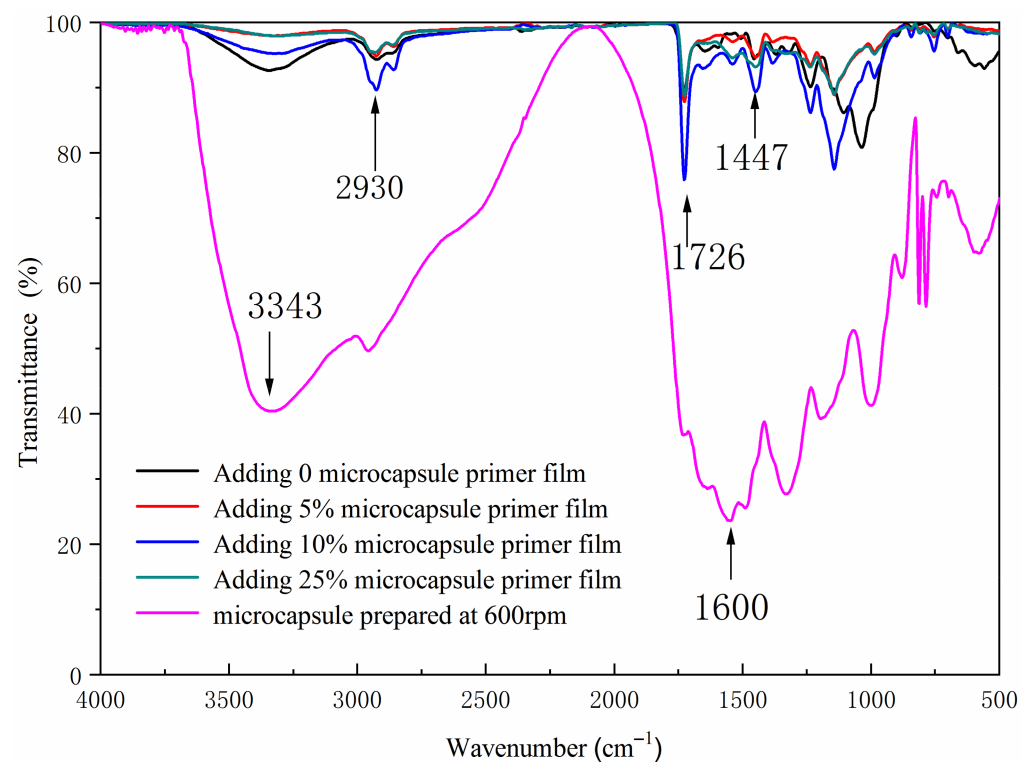


Figure 9. The FTIR of primer film with different microcapsule concentration.

3.6. Effect of Microcapsules on Aging Resistance of Surface Coating on *Tilia europaea* L. Wood

According to the mechanical, optical and liquid resistance test results, the film prepared by adding 5.0% concentration of microcapsules (obtained at 600 rpm stirring rate) had better performance. *Tilia europaea* L. film without microcapsules and with 5.0% microcapsules (obtained at 600 rpm stirring rate) was ultraviolet aged for 24 h. The influence of aging time on the color difference of paint film is shown in Table 9. The value of a^* in the table represents the red green value. After aging, the value of a became smaller because the shellac was purplish red, which indicated that ultraviolet light had an effect on the color of shellac. After UV aging, the color difference of *Tilia europaea* L. film with microcapsule was smaller than that without microcapsule, which indicated that the aging resistance of *Tilia europaea* L. film with microcapsule was stable after UV irradiation.

Table 9. Color difference after UV aging.

Aging Environment	Microcapsule Concentration (%)	Aging Time (h)	L^*	a^*	b^*	c^*	H^*	ΔE^*
UV	0	0	63.0 ± 2.4	17.1 ± 0.2	29.1 ± 0.7	34.1 ± 0.5	58.6 ± 1.3	-
		24	54.2 ± 1.6	15.1 ± 0.3	22.2 ± 1.1	26.9 ± 0.5	55.7 ± 1.7	11.3 ± 0.2
	5.0	0	70.7 ± 2.1	13.3 ± 0.3	20.7 ± 0.6	24.6 ± 0.9	57.3 ± 1.5	-
		24	64.0 ± 1.9	13.1 ± 0.4	17.2 ± 0.4	21.6 ± 0.4	52.6 ± 1.8	7.5 ± 0.2

Table 10 shows the effect of microcapsule on the gloss of waterborne primer film before and after aging. The gloss of coating after UV aging was lower than that before aging, and the gloss of coating with microcapsules was lower than that without microcapsule.

Table 10. Gloss change after UV aging.

Microcapsule Concentration (%)	Aging Time (h)	20°	60°	80°
0	0	2.0 ± 0.1	5.1 ± 0.1	3.1 ± 0
	24	1.9 ± 0	4.9 ± 0.1	2.1 ± 0
5.0	0	1.8 ± 0	4.7 ± 0.2	3.0 ± 0
	24	1.3 ± 0	3.1 ± 0	1.5 ± 0

The SEM of coating without microcapsules and with 5.0% microcapsules before and after aging are shown in Figure 10. The coating without microcapsule was smooth before aging, and had a large range of irregular round cracks after UV aging. The coating with 5.0% microcapsules had fine particles before aging and round cracking after UV aging, but the cracking diameter was smaller than that without microcapsules, which indicated that microcapsules could delay the aging of the film.

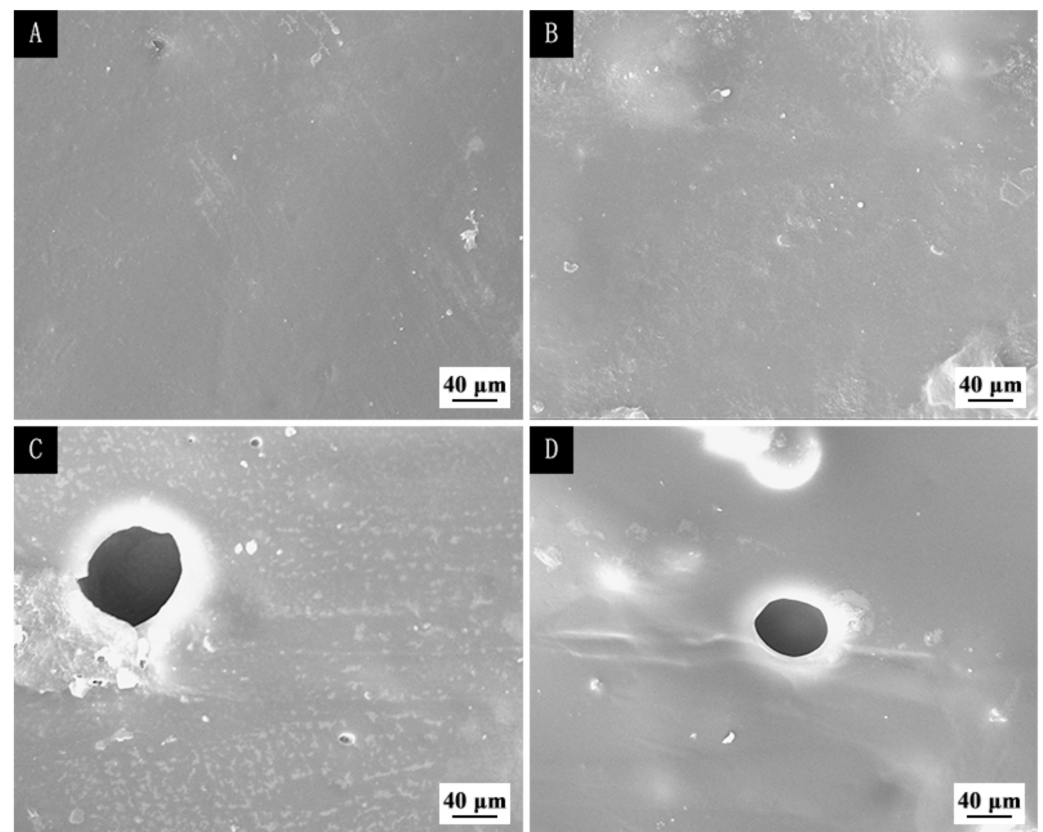


Figure 10. The SEM of waterborne primer film with different concentration of microcapsules (600 rpm stirring rate) before and after aging: before aging, (A) 0%, (B) 5.0%, after aging, (C) 0%, (D) 5.0%.

Figure 11 shows the FTIR of the film with and without microcapsules before and after aging. The characteristic absorption peaks of functional groups in each substance are shown in Table 10. No peaks disappeared before and after aging, indicating that there was no difference in the composition of the film before and after aging. The results showed that the aging environment had no effect on the composition of the film with or without 5.0% microcapsules.

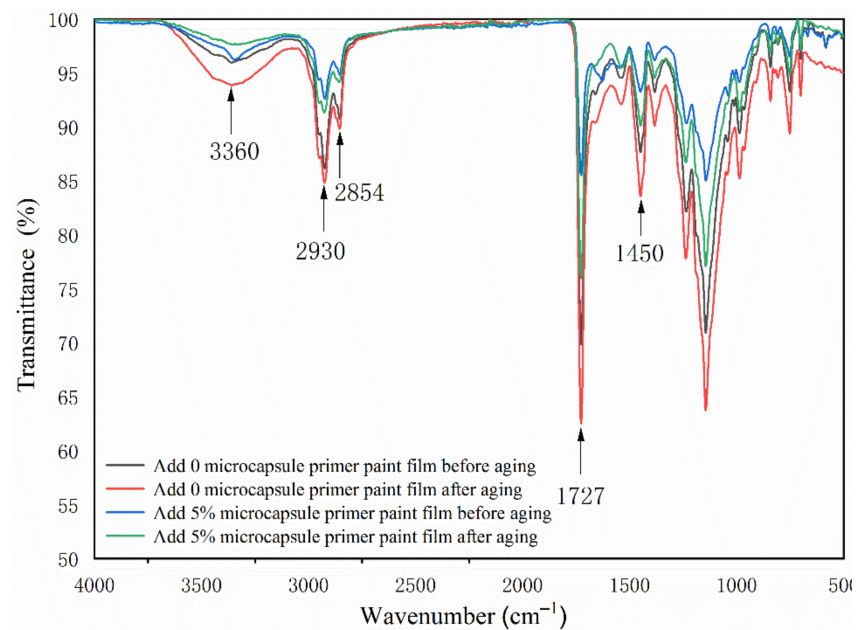


Figure 11. The FTIR of coatings with different concentration of microcapsules before and after UV aging.

3.7. Effect of Microcapsules on the Self-Healing Properties of Surface Coating on *Tilia europaea* L. Wood

The paint film scratch repair diagram is shown in Figure 12. After 7 days of repair, the scratch of paint film with 5.0% microcapsules (prepared at 600 rpm stirring rate) was reduced from 16.50 μm to 10.05 μm , whose repair rate was 39.0% and the scratch of paint film with 10.0% microcapsules (prepared at 600 rpm stirring rate) was reduced from 15.86 μm to 9.35 μm . The results showed that the microcapsule of MF resin coated shellac and waterborne coating had a certain repairing effect on the coating. In [32], a waterborne acrylic coating was used as the core material of the microcapsule, and the crack of the self-healing coating was reduced from 10.59 μm to 8.40 μm . The repair rate of the coating was 20.6%, which was lower than that of the coating with shellac and waterborne coating as the core material. Because of the strong adhesion of shellac resin, the repairing effect of shellac mixed with waterborne coating was higher than that of waterborne coating itself.

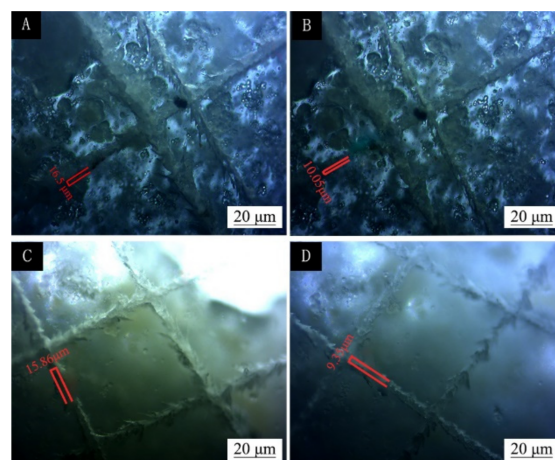


Figure 12. The OM of waterborne primer film with different concentration of microcapsules (600 rpm stirring rate) before and after repair: (A) and (B) before and after the repair of 5.0% microcapsules, (C) and (D) before and after the repair of 10.0% microcapsules.

4. Conclusions

The color difference of waterborne primer on *Tilia europaea* L. surface was the smallest when the concentration of microcapsules prepared at 600 rpm was 10.0%. When the concentration of microcapsule was 5.0%, the gloss of the film was higher. When the concentration of microcapsules prepared at 600 rpm was 5.0%, the film elongation at break was the highest. The film with 5.0% microcapsule had better adhesion, and the film with 5.0% and 10.0% microcapsule concentration had better hardness. The impact resistance of the film first increased and then decreased with the rise of microcapsule concentration. The gloss of paint film after liquid resistance of red ink was lower than that of NaCl, ethanol and detergent. In the aging test, the color difference of the film with microcapsule was smaller than that without microcapsule, and the self-healing effect of the coating was better when the concentration of microcapsule is 5.0%. The results provide a useful technical reference for wood coating repair.

Author Contributions: Conceptualization, methodology, validation, resources, data management, supervision, X.Y.; Formal analysis, investigation, writing-review and editing, Y.T., Investigation and writing-review, Y.C. All authors have read and agreed to the published version of the manuscript.

Funding: This project was partly supported by the Natural Science Foundation of Jiangsu Province (BK20201386) and Youth Science and Technology Innovation Fund of Nanjing Forestry University (CX2016018).

Institutional Review Board Statement: Not applicable.

Informed Consent Statement: Not applicable.

Data Availability Statement: Not applicable.

Conflicts of Interest: The authors declare no conflict of interest.

References

1. Ullah, H.; Azizli, K.A.M.; Man, Z.B.; Ismail, M.B.C.; Khan, M.I. The potential of microencapsulated self-healing materials for microcracks recovery in self-healing composite systems: A review. *Polym. Rev.* **2016**, *56*, 429–485. [[CrossRef](#)]
2. Chen, M.F.; Fan, D.C.; Liu, S.M.; Rao, Z.L.; Dong, Y.L.; Wang, W.X.; Chen, H.; Bai, L.J.; Cheng, Z.P. Fabrication of self-healing hydrogels with surface functionalized microcapsules from stellate mesoporous silica. *Polym. Chem.* **2019**, *10*, 503–511. [[CrossRef](#)]
3. Zhang, C.B.; Gao, W.; Zhao, Y.J.; Chen, Y.P. Microfluidic generation of self-contained multicomponent microcapsules for self-healing materials. *Appl. Phys. Lett.* **2018**, *113*, 203702. [[CrossRef](#)]
4. Niu, R.W.; Jin, M.L.; Cao, J.P.; Yan, Z.B.; Gao, J.W.; Wu, H.; Zhou, G.F.; Shui, L.L. Self-healing flexible conductive film by repairing defects via flowable liquid metal droplets. *Miromachines* **2019**, *10*, 113. [[CrossRef](#)]
5. Feng, H.Y.; Yu, F.; Zhou, Y.; Li, M.; Xiao, L.H.; Ao, Y.H. Fabrication of microcapsule-type composites with the capability of underwater self-healing and damage visualization. *RSC Adv.* **2020**, *10*, 33675–33682. [[CrossRef](#)]
6. Song, Y.K.; Kim, B.; Lee, T.H.; Kim, J.C.; Nam, J.H.; Noh, S.M.; Park, Y.I. Fluorescence detection of microcapsule-type self-healing, based on aggregation-induced emission. *Macromol. Rapid Comm.* **2017**, *38*, 1600657. [[CrossRef](#)]
7. Yan, X.; Qian, X.; Chang, Y. Preparation and characterization of urea formaldehyde @ epoxy resin microcapsule on waterborne wood coatings. *Coatings* **2019**, *9*, 475. [[CrossRef](#)]
8. Tan, X.Y.; Zhang, J.P.; Guo, D.; Sun, G.Q.; Zhou, Y.Y.; Zhang, W.W.; Guan, Y.S. Preparation, characterization and repeated repair ability evaluation of asphalt-based crack sealant containing microencapsulated epoxy resin and curing agent. *Constr. Build. Mater.* **2020**, *256*, 119433. [[CrossRef](#)]
9. Ma, L.L.; Shang, Y.N.; Zhu, Y.D.; Zhang, X.N.; Jingjing, E.; Zhao, L.H.; Wang, J.G. Study on microencapsulation of lactobacillus plantarum LIP-1 by emulsification method. *J. Food Process. Eng.* **2020**, *43*, e13437. [[CrossRef](#)]
10. Khodabakhshghadam, S.; Khoshfetrat, A.B.; Rahbarghazi, R. Alginate-chitosan core-shell microcapsule cultures of hepatic cells in a small scale stirred bioreactor: Impact of shear forces and microcapsule core composition. *J. Biol. Eng.* **2021**, *15*, 14. [[CrossRef](#)]
11. Fan, C.J.; Zhou, X.D. Influence of operating conditions on the surface morphology of microcapsules prepared by in situ polymerization. *Colloid. Surface. A* **2010**, *363*, 49–55. [[CrossRef](#)]
12. Schultz, S.; Wagner, G.; Urban, K.; Ulrich, J. High-pressure homogenization as a process for emulsion formation. *Chem. Eng. Technol.* **2004**, *27*, 361–368. [[CrossRef](#)]
13. Knupfer, P.; Ditscherlein, L.; Peuker, U.A. Nanobubble enhanced agglomeration of hydrophobic powders. *Colloid. Surface. A* **2017**, *530*, 117–123. [[CrossRef](#)]
14. Mozaffari, S.M.; Beheshty, M.H.; Mirabedini, S.M. Effect of processing conditions on the microencapsulation of 1-methylimidazole curing agent using solid epoxy resins. *Iran. Pol. J.* **2017**, *26*, 629–637. [[CrossRef](#)]

15. Zhang, C.; Wang, H.R.; Zhou, Q.X. Preparation and characterization of microcapsules based self-healing coatings containing epoxy ester as healing agent. *Prog. Org. Coat.* **2018**, *125*, 403–410. [[CrossRef](#)]
16. Wang, Q.P.; Cao, J.Z.; Liu, X.E.; Yang, S.M.; Jiang, M.L. Self-healing coatings for inhibiting corrosion of ferrous metals exposed to preservative-treated bamboo. *J. Wood Sci.* **2020**, *66*, 18. [[CrossRef](#)]
17. Wang, H.R.; Zhou, Q.X. Evaluation and failure analysis of linseed oil encapsulated self-healing anticorrosive coating. *Prog. Org. Coat.* **2018**, *118*, 108–115. [[CrossRef](#)]
18. Pedaballi, S.; Li, C.C.; Song, Y.J. Dispersion of microcapsules for the improved thermochromic performance of smart coatings. *RSC Adv.* **2019**, *9*, 24175–24183. [[CrossRef](#)]
19. Zandi, M.S.; Hasanzadeh, M. The self-healing evaluation of microcapsule-based epoxy coatings applied on AA6061 Al alloy in 3.5% NaCl solution. *Anti-Corros. Method. Mater.* **2017**, *64*, 225–232. [[CrossRef](#)]
20. Durmaz, S.; Ozgenc, O.; Avci, E.; Boyaci, I.H. Weathering performance of waterborne acrylic coating systems on flat-pressed wood-plastic composites. *J. Appl. Polym. Sci.* **2020**, *137*, 48518. [[CrossRef](#)]
21. Wu, Y.; Wu, J.M.; Wang, S.Q.; Feng, X.H.; Chen, H.; Tang, Q.W.; Zhang, H.Q. Measurement of mechanical properties of multilayer waterborne coatings on wood by nanoindentation. *Holzforschung* **2019**, *73*, 871–877. [[CrossRef](#)]
22. Li, J.; Shan, W.W.; Cui, J.C.; Qiu, H.X.; Yang, G.Z.; Zheng, S.Y.; Yang, J.H. Enhanced corrosion resistance and weathering resistance of waterborne epoxy coatings with polyetheramine-functionalized graphene oxide. *J. Coat. Technol. Res.* **2020**, *17*, 171–180. [[CrossRef](#)]
23. Yu, J.F.; Pan, H.X.; Zhou, X.D. Preparation of waterborne phosphated acrylate-epoxy hybrid dispersions and their application as coil coating primer. *J. Coat. Technol. Res.* **2014**, *11*, 361–369. [[CrossRef](#)]
24. Liu, Q.Q.; Gao, D.; Xu, W. Effect of sanding processes on the surface properties of modified Poplar coated by primer compared with Mahogany. *Coatings* **2020**, *10*, 856. [[CrossRef](#)]
25. Liu, Q.Q.; Gao, D.; Xu, W. Influence of the bottom color modification and material color modification process on the performance of modified Poplar. *Coatings* **2021**, *11*, 660. [[CrossRef](#)]
26. Hu, J.H.; Li, Y.; Yi, L.; Guo, H.W.; Li, L. Evaluation of the dyeing properties of basswood veneer treated by dichlorotriazine reactive dye based on gray correlation analysis. *BioResources* **2016**, *11*, 466–481. [[CrossRef](#)]
27. Yang, H.M.; Yu, L.; Wang, L.H. Effect of moisture content on the ultrasonic acoustic properties of wood. *J. Forestry Res.* **2015**, *26*, 753–757. [[CrossRef](#)]
28. Bousack, H.; Kahl, T.; Schmitz, A.; Schmitz, H. Towards improved airborne fire detection systems using beetle inspired infrared detection and fire searching strategies. *Micromachines* **2015**, *6*, 718. [[CrossRef](#)]
29. Wu, S.S.; Tao, X.; Xu, W. Thermal conductivity of Poplar wood veneer impregnated with graphene/polyvinyl alcohol. *Forests* **2021**, *12*, 777. [[CrossRef](#)]
30. Mei, S.; Han, P.P.; Wu, H.; Shi, J.F.; Tang, L.; Jiang, Z.G. One-pot fabrication of chitin-shellac composite microspheres for efficient enzyme immobilization. *J. Biotechnol.* **2018**, *266*, 1–8. [[CrossRef](#)]
31. Zhou, J.; Yang, L.; Wang, X.L.; Fu, Q.J.; Sun, Q.L.; Zhang, Z.Y. Microencapsulation of APP-I and influence of microencapsulated APP-I on microstructure and flame retardancy of PP/APP-I/PER composites. *J. Appl. Polym. Sci.* **2013**, *129*, 36–46. [[CrossRef](#)]
32. Yan, X.; Zhao, W.; Qian, X. Effect of water-based emulsion core microcapsules on aging resistance and self-repairing properties of water-based coatings on Linden. *Appl. Sci.* **2021**, *11*, 4662. [[CrossRef](#)]